Mechanical and Environmental Tests of Brazed Ceramic Multilayer Packages

Brazing factors were systematically varied to study their effect on the macro and microstructure of a brazed joint

BY D. A. WEIRAUCH, JR.

ABSTRACT. Kovar pins were attached to tungsten-metallized, alumina ceramic packages with Ag-Cu alloys using a wide range of brazing process parameters that were systematically varied in a designed experiment. The impact of the brazing thermal process, furnace atmosphere, brazing filler metal composition, and brazing filler metal quantity on the performance of ceramic pin-grid arrays was assessed through mechanical and environmental tests. Metallographic analyses revealed that a wide range of brazement microstructure, macrostructure, and base metal interaction were produced. Nevertheless it was found that these divergent conditions had no detrimental effect on the cofired ceramic performance as judged by the results of pin-pull tests after exposure to vibrational fatigue, thermal shock, salt-spray corrosion, and temperature-humidity cycling. The lack of ceramic degradation, despite exposure to more severe brazing conditions than previously reported in the literature, is attributed to the combined quality of the package design, the materials set, and the fabrication processes.

Introduction

Thirty-eight percent of the total sales of advanced ceramics in 1991 were accounted for by capacitors, substrates and packages (Ref. 1). Electronic packaging of semiconductor devices encompasses the designs and interconnection technologies that provide the electrical, thermal, mechanical and chemical environment required for the proper functioning of micron-scale integrated circuits fabricated on silicon chips. Comprehensive overviews of this technology are available elsewhere (Refs. 2, 3). Packaging is the most important application of ceramics in microelectronics, with ceramics accounting for roughly two-thirds of the total packaging market in 1987 (Ref. 4). Metal lines, frequently defined using thick-film technology, are buried within the ceramic body and provide the electrical interconnection between the integrated circuit and the next level in the electronic system. The predominance of ceramics as the dielectric material is related to their unique combination of electrical, mechanical, thermal and dimensional properties.

One manufacturing technology commonly used for the production of multilayer ceramic packages is the high-temperature cofire process. The high sintering temperatures (1550°–1650°C; 2822°–3002°F) of the alumina-glass dielectric material necessitates the use of refractory metals such as tungsten or molybdenum as the conductors. Multilayer structures are built through a multistep process involving: 1) dispersing the inorganic powders into an organic solvent-binder system to a consistency of paint; 2) casting the paints into 200–250-micron (0.0079–0.0098-in.) thick, flexible tape; 3) blanking the tape into cards; 4) punching and filling holes in the cards with the conductor ink; 5) screen-printing the electrical circuitry on individual cards; 6) stacking and laminating individual cards; 7) firing in a reducing atmosphere; 8) initial plating and I/O pin brazing; and 9) finish plating (Ref. 2).

KEY WORDS

Furnace Brazing
Kovar
Metallized Alumina
Ceramic Package
Ceramic Pin-Grid Array
Process Parameters
Mechanical Tests
Environmental Tests
Microstructure
Pin-Pull Strength

Ag-Cu alloys provide the appropriate temperature hierarchy for the attachment of Alloy 42 or Kovar I/O pins by furnace brazing (Ref. 5). The initial plating forms a secondary metallizing layer, which aids the wetting of the refractory metal by the braze alloy while minimizing the penetration of the braze into the thick-film metallization (Ref. 6). The flow of the brazing filler metal on the Ni-plated, tungsten metallization has been assessed by area-of-spread measurements and hot-stage microscopy as described elsewhere (Refs. 7–9). As little as 0.25 microns of electroplated Ni results in brazed joints of acceptable strength. The final plating ensures a reliable electrical contact is formed when the assembled package is inserted into the electronic system.

The attachment of Kovar leads to ceramic packages by furnace brazing has been reported in the literature to have an adverse effect on the mechanical properties of cofired ceramic packages (Refs. 10, 11). In one of these studies, the brazing operation was shown to decrease the

D. A. WEIRAUCH, JR., is with the Electronic Packaging Center, Alcoa Technical Center, Alcoa Center, Pa.

Table 1—The Six Factors of the Brazing Experiment and Their Ranges

Filler Alloy Composition	Ag-15 Cu	Ag-28Cu
Peak Temperature (±7°C)		
High	955	955
Low	888	809
Time above 780°C (±0.6 min)		
High	9.5	9.5
Low	1.5	1.5
Furnace Atmosphere (% H_2)		
High	100	100
Low	0	0
Filler Alloy Quantity (mg/2.128 mm² braze pad)		
High	1.5	1.5
Low	0.5	0.5
PGA Substrate Cleaning	as-received cleaned	as-received cleaned

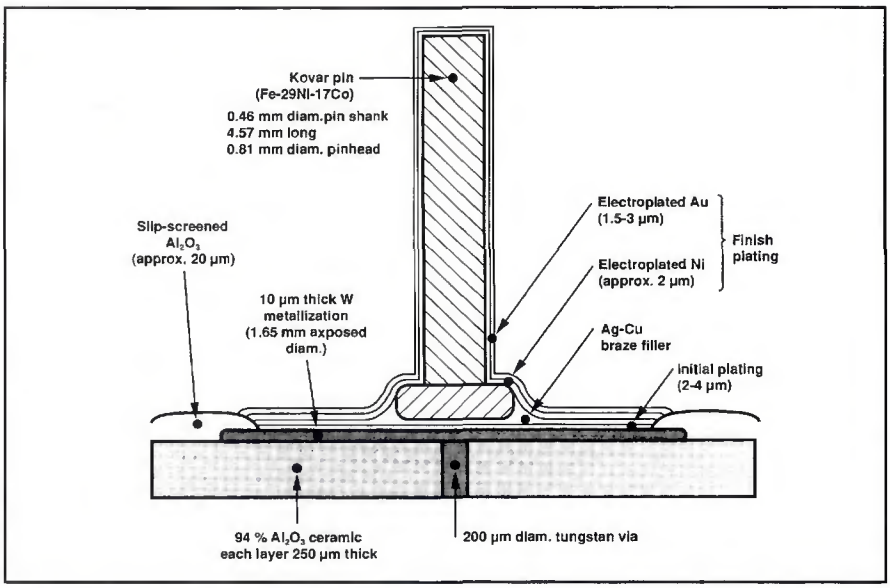

Fig. 1 — Schematic section through a brazed joint.

mean flexure strength of cofired alumina packages (Ref. 11). In the other study, various aspects of the joint design (fillet morphology, pinhead diameter, and metallized braze pad diameter) were shown to affect the strength of the joint through the level of residual stress (Ref. 10). Additionally, certain conditions of materials and processing have been reported to lead to liquid-metal corrosion (Refs. 12–16) and stress-corrosion cracking (SCC) of Kovar (Refs. 14, 15, 17, 20–22). Considerable controversy remains over the importance of specific processes and mechanisms. Weirick (Ref. 14) cited the presence of a tensile stress, insufficient nickel plating on Kovar, grain boundary penetration of Kovar by Cu, and the presence of contaminants containing free chlorides as factors that contributed to SCC. By contrast, Vaughan (Ref. 16) and Fuerschbach (Ref. 23) found no deleterious effect related to the penetration of Kovar grain boundaries by Cu. Rosengarth (Ref. 17) observed intergranular penetration of Kovar by both Cu and Ag. He further observed that intergranular penetration occurring during brazing is a localized corrosion phenomenon and not necessarily associated with LME as concluded by previous researchers (Refs. 13, 14, 16). Fuerschbach (Ref. 23) cautioned that preplating Kovar with Ni can cause increased environmental degradation (pitting corrosion and cracking) when eutectic Ag-Cu brazes are used.

In this study, Kovar pins were attached to tungsten-metallized, alumina ceramic packages with Ag-Cu alloys. Major brazing process factors were systematically varied in a designed experiment to assess their impact on the the subsequent performance of ceramic pin-grid arrays (PGA) in mechanical and environmental tests. Brazing furnace atmosphere and thermal profile, filler metal composition and quantity, and substrate precleaning were chosen as variables likely to affect the microstructure and macrostructure of the brazed joint. The macrostructure of the brazed joint was considered to be of importance for several reasons. First, the fillet geometry is known to affect the level of residual stress in the brazed joint (Refs. 10, 24). Excessive accumulation of braze around the pinhead perimeter can lead to a decrease in the strength of the joint. Secondly, qualitative issues pertaining to workmanship (surface roughness, stains, corrosion resistance) are monitored by the electronics industry even if they have no direct relation to functional failures. Rough surfaces can trap plating solutions or lead to pores, which result in corrosion sites during proof testing (Ref. 25). Since no systematic data were available for the interrelation of brazed joint surface finish with the corrosion resistance of overplated, brazed joints, they were included as additional factors in this study.

Materials

A schematic representation of a brazed pin joint on a multilayer ceramic package is shown in Fig. 1 along with some of the key materials and their approximate dimensions. The key materials are the Kovar (Fe-17Ni-7Co) input-output (I/O) pin, the Ag-Cu brazing filler metal, and the nickel-plated tungsten brazing pad. The brazing fixtures were machined from Poco Graphite[1]. The test vehicle in this study was a ten-layer, 132 I/O pin count pin-grid array package with 0.065-in. (1.65-mm) diameter brazing pads on 0.100-in. (2.54-mm) centers — Fig. 2. Cofired tungsten 94% Al_2O_3 PGAs were produced by the process described above. An electrolytic nickel-sulfamate plating was applied to all exposed tungsten metallization prior to brazing.

The composition of the Ag-Cu brazing filler metal was either a near-eutectic (72 wt-% Ag- 28 wt-% Cu) or a hypoeutectic (85 wt-% Ag-15 wt-% Cu). The liquidus temperature of the eutectic composition is 780°C (1436°F), while the liquidus and solidus temperatures of the hypoeutectic are 845° and 780°C (1553° and 1436°F), respectively. These two compositions are commonly used in this application and were expected to give a reasonable assessment of the effect of brazing filler metal composition on Kovar attack. The pins were purchased with 0.5-, 1.0-, and 1.5-mg claddings of brazing filler metal in the form of hemispheres attached by furnace reflow[2]. During the brazing

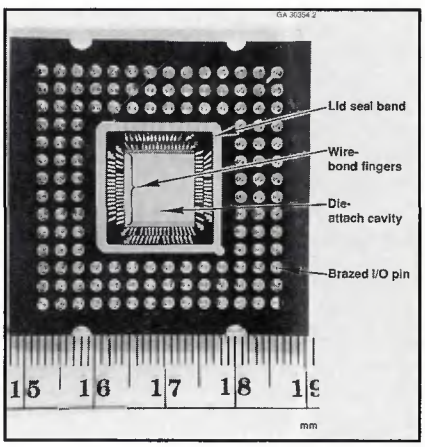

Fig. 2 — Photograph of a 132-pin PGA used as the test vehicle.

1. Grade DFP-1, Poco Graphite, Inc., Decatur, Tex.

2. Sumitomo Special Metals Co., Ltd., Japan.

Table 2 — Description of the Six Main Experimental Responses

1. Metallography	
Objective:	Characterization of the chemistry, macrostructure, microstructure and phase distribution of the components of the brazed joint (pin, fillet, base metal).
Procedure:	Polished vertical section through brazed joint, optical microscope and SEM views of parts prior to sectioning.
Criteria:	Fillet geometry, brazed joint microstructure, fillet surface roughness, base metal microstructure (pin and metalization).
2. Pin-Pull Tests	
Objective:	Determine the mechanical integrity of the as-brazed joints.
Procedure:	tensile pull and 20-deg pull—Instron.
Criteria:	Level of applied force at failure and failure mode.
3. Vibration (variable frequency)	
Objective:	Determine the effect of vibration on the brazed joint over various frequency ranges. Assess potential weakening of the joint due to stress-corrosion cracking or liquid metal embrittlement of the Kovar pins.
Procedure:	MIL Std. 883-C, Method 2007.1, Condition A—20-g peak acceleration.
Criteria:	Inspection for cracking, degradation of pull strength.
4. Thermal Shock Resistance	
Objective:	Determine the ability of the brazed joint to withstand sudden exposure to extremes in temperature.
Procedure:	MIL Std. 883-C, Method 1011, Condition C: 100 cycles between liquids at −65° and 150°C.
Criteria:	Evidence of cracking of the ceramic in near the braze pad as determined by optical or SEM inspection, and degradation of pull strength.
5. Moisture Resistance	
Objective:	Evaluate plating structure for defects or porosity in Au and Ni plating.
Procedure:	Evaluate stress-corrosion cracking of Kovar pins.
Criteria:	MIL Std. 883-C, Method 1004.4: 10 continuous 24-h cycles from 25° to 65°C at 90–100% RH. Insulation resistance, corrosion bridges or products, degradation of pin-pull strength.
6. Salt Spray Corrosion	
Objective:	Evaluate the corrosion resistance of the package metallic components in a severe environment (*i.e.*, NaCl fog).
Procedure:	MIL Std. 883-C, Method 1009.6, ASTM B117-85. 2.5% NaCl fog, 35°C, 24 and 48 h.
Criteria:	% of metal area covered with corrosion products, 90-deg bend test of pins.

process, these volumes of filler metal flow to the perimeter of the 0.00332-in.^{2} (2.128 mm^2) brazing pad, as well as part way up the head of the I/O pin forming joints with distinct fillet geometries.

Experimental Design

Response surface methodology provides a disciplined and systematic approach to evaluating the results of experiments involving multiple variables (Refs. 26–28). A common statistical approach to experimental designs involves the use of factorial structures. A number of experiments required for a complete two-level (main effect) factorial involving "n" variables is 2^n. Important features of the factorial design are that the extreme values of the variables are included and interactions between variables can be determined. When the number of variables is large, screening designs can be employed to hold the number of experiments to a manageable level and still obtain a reasonable estimate of interactions between variables. The best estimate of experimental variability results from repeating or replicating experiments in randomized run order at every point in experimental space. An alternative, more efficient approach is to only replicate runs at the center of the experimental space defined by the "n" variables.

A six-factor interaction design in 32 trials was chosen for this experiment. This is half of a full two-level factorial design for six factors. The high and low values (range) of each variable used in this experiment are shown in Table 1. As discussed in the next section, the range of thermal cycles used for the two brazing filler metals was shifted to account for the different phase relationships. Assessment of variability between each set of eight parts was made possible by replicating a run near the center point of the experimental space. These midpoint values (run numbers 1, 19, 35 and 38 in Table 3) are near the true center point of the experimental space since only two levels of the filler metal were used. Center point values for the other factors were run separately for each alloy. This translated to six runs to generate the three center point replicates. Ceramic packages were brazed in each of the 32 trials. One package was used for each of the six main responses listed in Table 2. Since there were 132 brazed pin joints on each package, the sample size ranged from four pin joints (metallography or mechanical tests) to 132 (environmental tests). This experimental design and subsequent data analysis were conducted with commercially available software[3].

The six major responses are listed in Table 2. In actuality, some of the major responses have more than one measurable criterion, so the total number of responses is greater than six.

Experimental Procedure

Pins were attached to the ceramic packages by furnace brazing using a continuous-belt hydrogen furnace[4]. The proper settings of belt speed, and temperature on the three zones of the furnace for all of the desired experimental points were established by the monitoring of Type K traveling thermocouples embedded at various positions in the graphite fixtures. One standard deviation around temperature (based on a minimum of 12 measurements) was typically under seven degrees, while the standard deviation for time above the eutectic was typ-

3. Strategy from Edgework, Inc., Seattle, Wash.

4. Model LA306, Radiant Technology Corp., Anaheim, Calif.

Table 3 — Run Table for the Brazing Experiment

Run Order	Run No.	Factor					
		Temp.	Time	$\%H_2$	%Cu	Amt.	Clean?
1	1	881	5.7	10	28	1.0	Y
2	2	963	10.1	0	15	1.5	N
3	3	882	2.75	100	15	0.5	N
4	4	814	1.7	100	28	1.5	N
5	5	964	5.1	100	15	1.5	N
7	6	970	6.2	0	28	1.5	Y
8	7	962	9.8	0	15	0.5	Y
9	8	966	4.8	100	28	1.5	Y
10	9	970	5.4	0	28	1.5	Y
11	10	958	9.3	100	28	1.5	N
12	11	814	1.6	100	28	0.5	N
13	12	817	1.7	0	28	1.5	Y
14	13	803	9.3	100	28	0.5	N
15	14	973	5.8	0	28	0.5	N
16	15	969	5.8	100	28	1.5	N
17	16	970	5.8	0	15	0.5	N
18	17	962	9.8	0	15	1.5	Y
19	18	811	10.6	0	28	0.5	N
20	19	892	4.4	10	28	1.0	Y
21	20	894	2.8	0	15	1.5	N
22	21	814	1.4	100	28	0.5	Y
23	22	971	5.6	0	15	1.5	Y
24	23	968	4.9	100	15	0.5	Y
25	24	889	2.9	0	15	0.5	Y
26	25	901	8.8	0	15	1.5	N
27	26	958	9.7	100	28	0.5	N
28	27	893	8.2	100	15	1.5	Y
29	28	898	8.7	0	15	0.5	Y
30	29	962	9.9	0	15	0.5	N
31	30	883	2.5	100	15	1.5	Y
32	31	955	9.8	100	15	1.5	Y
34	32	809	10.8	0	28	1.5	N
35	33	963	9.8	0	28	1.5	Y
36	34	956	9.9	100	15	0.5	N
37	35	886	4.3	10	28	1.0	Y
36	36	845	3.6	100	28	0.5	N
33	37	884	4.5	0	15	1.0	Y
38	38	883	4.3	10	15	1.0	N
39	39	889	4.4	100	15	1.0	Y
40	40	851	3.8	100	28	0.5	Y

Note: Temperatures and times are averages of four measurements for each run.

ically under 0.6 min. These averages included all the variation due to thermocouple position in the brazing fixture and run-to-run variability. A typical time-temperature profile is shown in Fig. 3.

Two key parameters are identified: peak temperature and time above the Ag-Cu eutectic temperature (780°C). The lowest time and temperature were set to be near the minimum for the braze to melt and flow. It is different for Ag-28Cu and Ag-15Cu largely due to phase relationships in the binary Ag-Cu system. The lowest peak brazing temperature used for the Ag-15Cu alloy was 882°C (1620°F), while that for the Ag-28Cu alloy was 809°C (1488°F). Therefore, both alloys were brazed using identical thermal cycles from the midpoint temperature (approximately 885°C ±7°) and higher.

Furnace atmosphere was varied from 100% H_2 to 100% N_2. A "forming gas" atmosphere (N_2-10H_2) was selected for the center point value and run off of compressed gas cyclinders. Pure H_2 and N_2 were drawn off of the laboratory gas lines. The moisture content of the gases was not measured. It has been shown to affect braze wetting and fillet formation for low-carbon steel plates brazed with copper pastes (Ref. 8). The writer is not aware of similar studies using silver brazing filler metals.

The quantity of brazing filler metal in the joint depended upon the starting

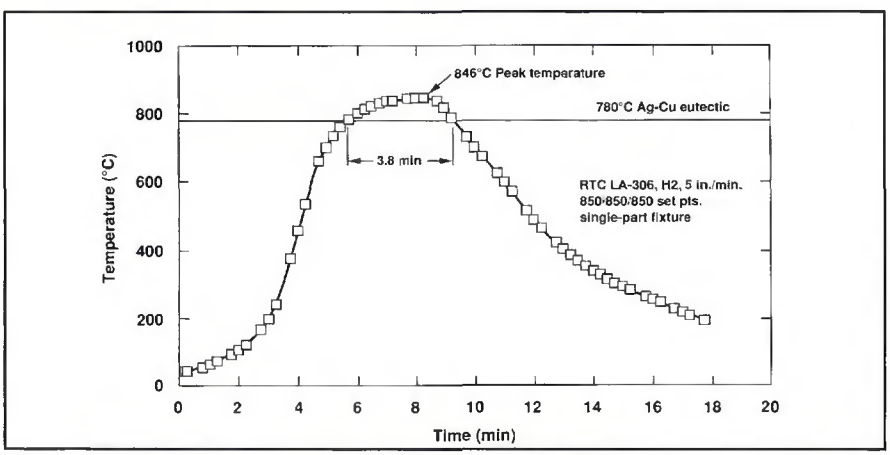

Fig. 3 — A typical brazing temperature profile.

5. Model 1122, Instron Corp, Canton, Mass.

6. Viking Labs/Honeywell, Mountain View, Calif.

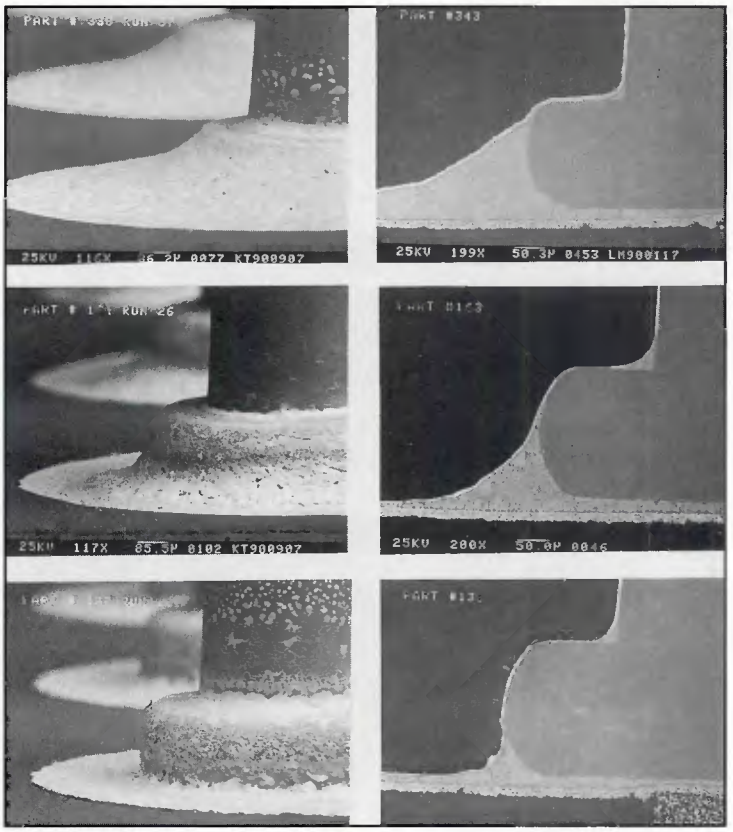

Fig. 4 — Examples of different fillet shapes. Brazing conditions are listed in Table 3. A — Run 37; B — Run 26; C — Run 1B.

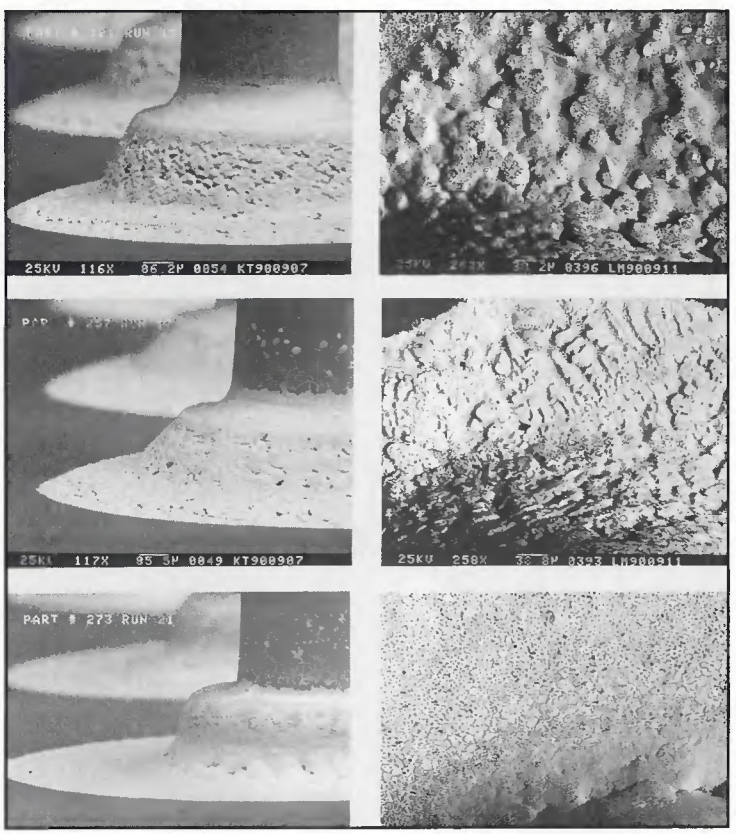

Fig. 5 — Examples of different fillet roughnesses. Brazing conditions are listed in Table 3. A — Run 15; B — Run 17; C — Run 21.

amount of cladding on the pins (0.5, 1.0 and 1.5 mg) and the extent of flow during brazing. During the brazing process, these volumes of brazing filler metal will flow to the perimeter of the 0.00332-in.^{2} (2.128-mm^2) braze pad, as well as part way up the head of the I/O pin, forming joints with distinct fillet geometries.

The final factor, substrate cleaning, also had no center point value. Half of the Ni-plated, tungsten-metallized, alumina substrates were cleaned prior to brazing with a procedure involving an initial detergent rinse, a water rinse, 10 to 15 s in 50% HCl at 63°C, additional hot and cold rinses in distilled, deionized water, and a final Freon solvent drying step (which assured that residual moisture content was not a problem). This cleaning was undertaken to assess the impact of removing loosely adherent debris that was picked up during package fabrication. Care was taken in subsequent part handling (such as the use of finger cots) to avoid sample contamination.

After brazing, final electroplates of Ni and Au were applied for corrosion protection, prior to metallographic examination and testing. Details of the plating chemistry are considered proprietary, but the approximate thicknesses are shown in Fig. 1. Since the performance of these packages in corrosion tests is strongly dependent on the protective nature of the coating, the plating process uniformity was carefully controlled.

An outline of the experimental runs conducted in this study is presented in Table 3.

Results

Fillet shape is important in that it affects the level of residual stress in the components of the brazed joint as well as the current distribution in final plating. The fillet shape was qualitatively assessed by examining the as-brazed fillets with SEM and optical microscopic techniques. A range of fillet shapes was produced in this study — Fig. 4. The fillet height, defined as the distance the braze climbed up the side of the Kovar pinhead, was used to correlate the brazing conditions to fillet shape. It is directly related to the wetting of the Kovar. The fillet height was determined from metallographic sections. Braze quantity and alloy composition were the strongest factors. The fillet height increased as the brazed quantity or the silver content of the filler metal increased. Brazing temperature, time and furnace atmosphere were not significant factors since the 95% confidence intervals built around their multiple regression coefficients included zero.

Braze fillet surface roughness was

monitored since rough surfaces can trap plating solutions or lead to pores, which result in corrosion sites during proof testing or cosmetic defects such as stains (Ref. 25). A range of as-brazed fillet surface roughnesses was produced in this study — Fig. 5. The surface roughnesses were rank ordered using SEM views of the solidified braze surfaces. This was very subjective since there are differences in surface pits and size of features, as well as variations in roughness from location to location on the fillet. Nevertheless, some general observations can be made. The coarsest fillet surfaces all resulted from 1.5 mg of filler metal. Atmosphere (H_2 or N_2) had no obvious effect on roughness. The coarsest fillets resulted from Profile 7 (highest temperature and intermediate time) using either Ag-28Cu or Ag-15Cu or Profile 8 (highest temperature and longest time). While a smooth fillet surface would seem most likely to result in uniform overplating and is cosmetically preferred, there was no direct correlation with the corrosion results, which are presented later. Therefore, the range of surface roughnesses achieved in this study does not affect the quality of the finish plating.

Various aspects of the braze fillet microstructure using Ag-Cu filler metals are worth mentioning. A sampling of the microstructures observed in this study is shown in Fig. 6. The size and amounts of phases in the brazed joint are dependent on initial alloy composition, the brazing thermal cycle and the cooling rate. There are three constituents of the microstructure: the two terminal solid solution phases (a silver-rich "alpha" phase, a copper-rich "beta" phase), and the eutectic mixture of the alpha and beta phases. The microstructure typical of the eutectic composition is usually seen near the central portion of the braze fillet — Fig. 6. There is much less of the eutectic constituent in the Ag-15Cu brazements than the Ag-28Cu — Fig. 6A and C. Furthermore, a comparison of Fig. 6A and B shows there is much less of the eutectic constituent in the Ag-28Cu brazement that has experienced a higher brazing temperature and longer hold time. There is a similar decrease in the amount of eutectic constituent in Ag-15Cu brazements as the brazing temperature increases, although the effect is much less pronounced. The eutectic microstructure is seldom seen under the pin head or in the thin layer of braze near the pad perimeter. In these locations, the microstructure is a mixture of the alpha phase and a (Ni, Cu) solid solution that forms by reaction of the Ag-Cu braze with Ni in the Kovar pin or the initial Ni plating layer. The size and distribution of these three constituents is also a function of filler metal quantity since the cooling rate is affected. While quantification of these constituents might be possible through image analysis, this has not been attempted in this study. Further discussion of the silver-copper eutectic transformation is provided elsewhere (Refs. 29, 30).

The extent of reaction of the alloy with the Kovar pin and the initial nickel plating on the tungsten metallization is also affected by brazing conditions. Nickel has limited solubility in liquid Ag-Cu alloys (Ref. 31). The 1.65-mm-diameter tungsten braze pad is typically plated with 1.5 microns of nickel. If all of this dissolved in 0.5 mg of Ag-28Cu alloy, the nickel content would be 19 wt-%. The equilibrium concentration of Ni in Ag-28Cu at 850°C is 1 wt-% (Ref. 31). Thus, partial dissolution of the nickel in the braze alloys is expected. SEM/EDX analyses show that the nickel that goes into solution in the brazing filler metal, either from the nickel plating or the Kovar, is associated with the beta copper phase. This is due to the similarities in atomic size, crystal lattice and electronic structure of nickel and copper. A layer of Ni-Cu is seen at both the braze-tungsten and braze-Kovar interfaces in metallographic sections. Electron microprobe analyses of liquid diffusion couple samples has confirmed that the (Ni-Cu) layer forms as a result of liquid diffusion prior to solidification.

The concern of liquid metal embrittlement and stress-corrosion cracking of Kovar when brazed with Ag-Cu alloys has been amply discussed in the literature (Refs. 13, 15, 17, 19). Earlier studies of the interaction of silver braze alloys with Kovar or Alloy 42 observed either copper (Ref. 15) or both copper and silver (Ref. 17) at corroded grain boundaries. Rosengarth (Ref. 17) concluded that the attack is not true liquid metal embrittlement (LME) as reported earlier (Ref. 13), but rather intergranular liquid metal corrosion. In this study, Ag is observed between the surfaces of Kovar grains and is interpreted as the early stages of grain boundary dissolution. There is less attack of the Kovar at the braze-Kovar interface observed for the Ag-15 Cu alloy than for the Ag-28 Cu alloy. Furthermore, the attack is more extensive at higher brazing temperatures. A possible explanation is that there is less liquid phase under isothermal equilibrium conditions in the Ag-Cu-Ni system as the Cu content of the alloy or temperature falls (Ref. 31). Local saturation of the molten alloy with Ni would slow the rate of grain boundary attack.

The grain size of the Kovar alloy is affected by the brazing process if the peak temperature and hold time are high enough. Figure 7 shows the extremes of this effect experienced in this study. The

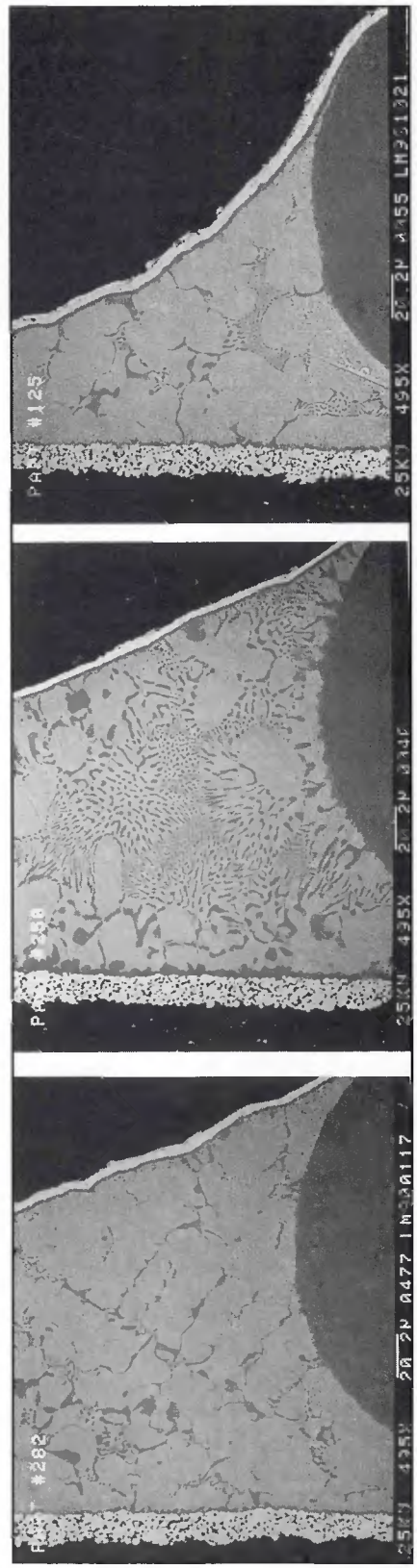

Fig. 6 — Examples of different fillet microstructures. A — Ag-28Cu, 969°C peak temp., 5.8 min above 780°C, H_2 atmosphere, 1.5 mg filler metal; B — Ag-28Cu, 817°C peak temp., 1.7 min above 780°C, N_2 atmosphere, 1.5 mg filler metal; C — Ag-15Cu, 971°C peak temp., 5.6 min above 780°C, N_2 atmosphere, 1.5-mg filler metal.

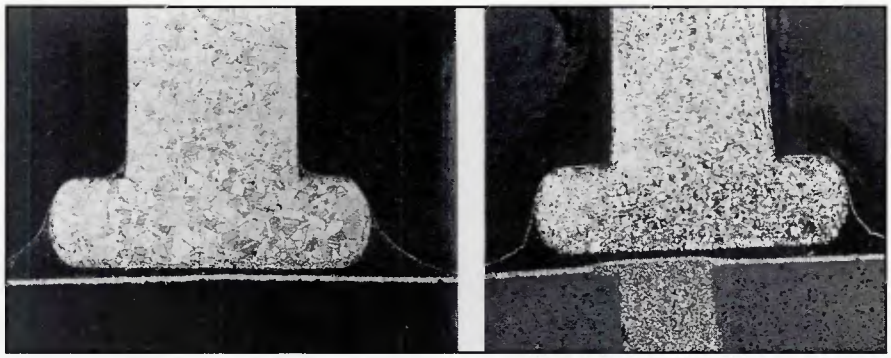

Fig. 7 — The effect of the brazing process on the Kovar pin microstructure. A — 958°C peak temp., 9.7 min above 780°C; B — 814°C peak temp., 1.6 min above 780°C.

microstructure has been revealed by a 20-s exposure to Marble's etchant. There is little change from the as-received microstructure in the sample, which was brazed with a 814°C (1499°F) peak temperature and an exposure time of 1.6 min above the eutectic temperature. However, there is considerable grain growth as evidenced by the large twinned grains in Fig. 7A after an exposure to a braze cycle with a 958°C (1757°F) peak temperature and 9.7 min dwell. The largest grains are approximately 11 microns in the low-temperature braze cycle compared to 80 microns in the high-temperature cycle, using a line intercept method. Increasing the grain size of the Kovar is a concern since it is expected to make the pins more susceptible to stress-corrosion cracking.

Mechanical Tests

Tensile tests were conducted on as-brazed samples in order to establish a background level of joint strength prior to environmental testing. A straight pull parallel to the pin shank axis was applied to selected pins from each package with an Instron mechanical testing unit[5]. In addition, a pull at an angle of 20 deg from the pin shank axis was applied, which combined bending and tension stresses. The latter is considered the more severe test as well as more representative of stresses likely to be experienced in service (Ref. 24). The Instron was run with a cross-head speed of 0.02 in./min. Two to four pins were tested from each package. There was no significant difference in pull strength due to the angle of loading — Table 4.

All of the joints broke near the middle of the pin shank. The pin shank diameter in this study is 0.018 in. (0.457 mm). If a load of 20.5 lb (9.30 kg) is applied, the applied engineering stress is 80,560 psi (5663.9 kg/cm^2 or 555.44 MPa), which is in agreement with the range of Kovar ultimate tensile strength specified by the vendor: 71,000–85,000 psi (490–586 MPa).

Environmental Tests

The premise that certain brazing conditions, such as high temperature and long hold time, would lead to degradation of the brazed joint strength was one of the motives for conducting this study. Consequently, in addition to visual inspection, the pull strengths of the brazed joints were determined after vibrational fatigue testing, thermal shock testing, and environmental corrosion testing.

The primary interest in vibrational fatigue testing was to determine if results similar to those of a previous study related to brazing Kovar lead frames to ceramic fine-pitch chip carriers were observed in this study (Ref. 19). They found that packages brazed with Ag-30 Cu fractured in the embrittled leads close to the brazement during vibration testing. The failure was attributed to a brazing temperature of 900°C (1652°F) where copper diffused along the Kovar grain boundaries and embrittled the leads. Samples brazed at 800°C (1472°F) in their study did not exhibit this failure. Vibrational fatigue testing of the multilayer ceramic packages from this study was conducted by an outside laboratory[6]. The tests involved a vibratory cycle sweeping from 20 to 2000 Hz and back to 20 Hz at a logarithmic rate such that no less than four min was required to complete a cycle. This is the procedure specified by MIL-STD 883C, although it is not known if the stress on the sample is enough to produce the deformation needed for fatigue. No visible fracturing was detected for any of the braze experiment PGAs after the vibrational test. Furthermore, pin-pull testing after vibrational exposure resulted in all pin failures at high loads in the range of 23 to 37 lb (10.43–16.78 kg). Thus, there was no significant degration in strength due to vibrational exposure when compared to the loads at failure for as-brazed PGAs, which ranged from 24 to 36 lb (10.89–16.33 kg).

The range of brazing conditions was much broader in the current study (higher temperatures and longer hold

Table 4 — Instron Pin-Pull Test Summary

Angle of Loading (to pin shank axis)	Load at Failure (lb)	1 Std. Dev.
parallel	20.5 (91.2N)	0.5 (139 d.f.)
20 deg	20.1 (89.4N)	0.7 (139 d.f.)

d.f. = degrees of freedom = number of observations −1.

times), yet there was no evidence of Kovar failure after vibrational fatigue testing. Differences in the Kovar microstructure is one possible reason for the conflicting results. In the previous work, the Kovar grains ranged in size from 10 to 29 microns, while those of this study ranged from 11 to 80 microns, depending on brazing thermal history — Fig. 7. A number of other differences between the two studies probably contributes to the differences in results. An additional factor is the level of residual stress in the Kovar lead, which depends on the extent of annealing after cold working. Flat leads and pins with heads might be expected to have different levels of strain due to forming differences; differences in annealing treatments are not known. In this study, the Kovar pins were obtained in the fully annealed condition. The Cu content of the brazing filler metal was 30% in the previous work and 28 or 15% in this study. Another difference is that the flat-lead packages were soldered to printed circuit boards prior to vibrational testing, and those of this study were not. Furthermore, MIL-STD 883C, method 2007, test condition A was used in this study, while their test conditions were different. Their samples would therefore experience different, and possibly more severe, stress states. This is probably the most important difference, which should be evaluated in a follow-up study.

Thermal shock testing was also conducted by an outside laboratory[6]. The details of the thermal cycle are outlined in Table 2. As found in vibrational fatigue testing, no visible fracturing was detected for any of the braze experiment PGAs after the thermal shock test. Again, 90-deg pin-pull testing after thermal cycling resulted in all pin failures (pin breakage or elongation) at high loads in the range of 26 to 36 lb (11.8–16.3 kg). Therefore, there was no degradation in strength due to this thermal cycling when compared to the loads at failure for as-brazed PGAs which ranged from 24 to 36 lb (10.9–13.3 kg).

A final check on ceramic damage due to the vibrational fatigue or thermal shock cycling was direct microscopic observation of the surface of cycled parts. Using a concept outlined elsewhere (Ref. 32), the pins and surface metallization

were chemically removed allowing direct inspection for surface cracks near the braze-pad perimeters. This procedure avoided possible cracking related to cross-section preparation. No evidence of cracking was observed in any of the samples.

Moisture resistance testing is a mild corrosion test and generally only reveals major problems (such as a porous or damaged finish plating). Only three of the 42 samples tested had any corrosion sites. Two had corrosion around the heads of brazed pins that had "hung up" in the brazing process. Visual examination of these parts at 65X before exposure revealed that the finish plating was very thin in these locations. The third sample had a patch of corrosion on the top-third of one pin shank. All of these corrosion sites can be related to unacceptable brazed joint formation or handling.

In salt spray corrosion testing, samples are held in an enclosed chamber and exposed to a "fog" of NaCl solution (Ref. 33). The MIL-STD 883C test allows for a 0.5 to 3.0% NaCl solution to be used, as well as varying exposure times, including 24, 48, 96 and 240 h. Test results vary from lab to lab, are dependent upon the orientation of the packages in the salt-spray chamber, and are sensitive to damage incurred during handling. For these reasons, less severe, as well as more realistic lab simulation tests, are being developed for evaluation of electronic material systems (Ref. 34). However, since these tests were not readily available and since many of the ceramic package customers require salt-spray testing to qualify product, the salt-spray test was used in this study.

The failure criteria of the salt spray test include the extent of corrosion products on metallized areas and a bend test for severely corroded areas. Based on the MIL-STD 883C, a part fails if there is "evidence of corrosion over more than 5% of the area of the finish or base metal of any package element" (*e.g.*, pins), or there is corrosion which "completely crosses the element." A pin might still fail if it exhibits electrochemical degradation such as pinholes, pitting, blistering, or flaking, and breaks or exposes base metal when bent through 90 deg at the most severely corroded site.

All of the parts had corrosion sites. Only four of the 40 samples tested failed the salt spray test with evidence of corrosion covering more than 5% of the finished metal area. The worst sample had corrosion sites on all 132 pins. A summary of the corrosion sites is recorded in Fig. 8. Most of the sites are on the pin shank, and the most of these near the middle third. Another sensitive site is the contact line where the pin shank joins the head of the pin. This site is even more significant when one considers the relatively small area involved. This might be related to a local thinning of the protective nickel and gold plating in this region. X-ray fluorescence and microsectioning measurements of plating thickness confirm the thinning. Models show that the primary current distribution results in thinner electrodeposits where the pin contour curves in, and they are thicker where there is an outward projection. Very little corrosion was observed on the braze fillet itself.

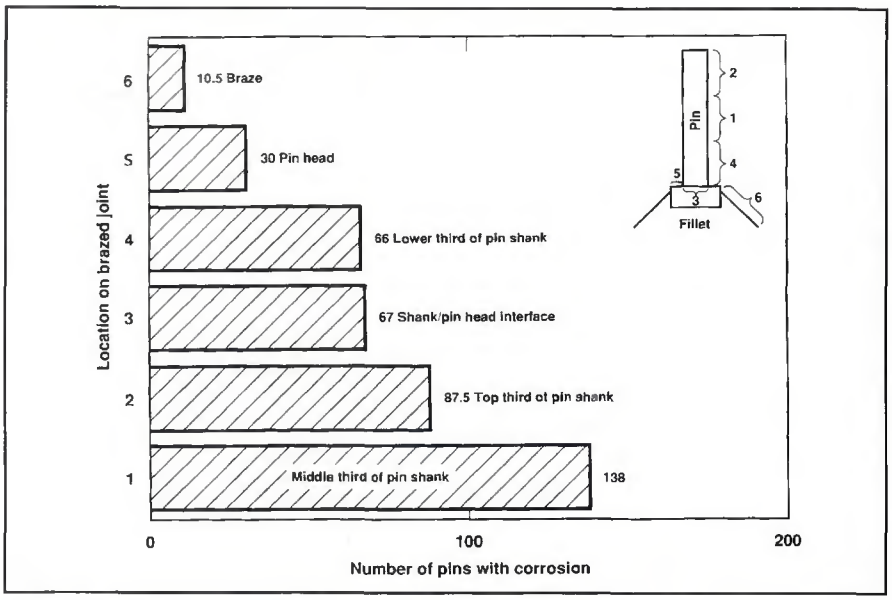

Fig. 8 — Salt spray corrosion site summary. Sample size of 40, 132-pin PGAs.

The structure of electrodeposits can be influenced by the nature of the substrate. The mimicking of the forms and boundaries of the substrate by the coating is known as pseudomorphism (Ref. 35). The continuation of the substrate structure for more than a few microns is rare in nickel deposits (Ref. 36). A systematic study of the effect of brazing conditions on changes in the nature of the Kovar substrate and its relation to plating defects has not been reported in the literature. Corrosion resistance was used as an indirect measure of the quality of the finish plating in this study.

The corrosion sites were separated into two groups for correlation with the brazing process parameters: pin corrosion sites and braze fillet sites. One-factor-at-a-time plots of these sites against brazing time, peak brazing temperature, braze quantity, braze furnace atmosphere, and alloy composition failed to yield any strong correlations. Multiple regression analysis likewise failed to yield a model that fits the data in a usable fashion. This lack of correlation of corrosion with the brazing process is significant since a range of Kovar grain size and braze fillet microstructure was observed in this study. The observed corrosion behavior is attributed to sample handling, test variability, or variability in the plating process itself.

In summary, the main mechanical and environmental responses had little or no dependence on any of the variables monitored. Joints of comparable performance were produced using either brazing filler metal, a variety of furnace atmospheres and a wide range of brazing thermal cycles. The optimum process should be selected to give uniform joints at the minimum brazing time and temperature. Other factors such as cost and safety of operation can be used to tailor the brazing process for specific needs.

Conclusions

Major changes in brazing process factors including the thermal cycle, furnace atmosphere, filler metal composition, and filler metal quantity have shown no detrimental effect on cofired ceramic package performance as judged by the results of metallographic inspection, and mechanical tests (pin-pull strength) performed on samples exposed to vibrational fatigue, thermal shock, salt spray corrosion, and temperature-humidity cycling. This robustness is attributed to the combined quality of the alumina-tungsten cofired ceramic materials, fabrication processes, brazing pins and package design. Salt spray corrosion results could not be correlated with any of the brazing factors. The observed corrosion behavior is attributed to sample handling, test variability, or variability in the plating process. Despite this high level of packaging system performance, product quality must be monitored as changes are made to any of the key packaging raw materials, processes, or design elements.

Acknowledgments

Special thanks are extended to W. Krafick for his careful and thorough experimentation, and L. Martin for the extensive characterization work and his interpretation of metallographic sections. J. Brassel, Z. Lipkes, M. Long and C. Rioflorido contributed to the selection of the key parameters for this study. P. Amstutz was instrumental in generating the large quantity of multilayer ceramic packages which formed the basis of this study. Those who contributed in substantial measure through direct participation in the present study include P. Bono, J. Capurso, P. Carey , E. Colvin, J. Horvath, A. Jaworski, S. Lee, K. Tipinski and P. Ziman. Finally, useful discussions throughout the course of this study were held with R. Burke, R. DiMilia, Z. Lipkes, M. Long, T. Luckie, B. Mogilevsky, K. Pahdy, D. Roha and B. Shabel. Completion of this study would not have been possible without the constant encouragement of R. DiMilia.

References

1. *Ceramics Industry*, 139 (3):27.

2. Seraphim, D. P., Lasky, R. C., and Li, C-Y. 1989. *Principles of Electronic Packaging*, New York, N.Y., McGraw-Hill.

3. Tummala, R. R., and Rymaszewski, E. J. 1989. *Microelectronic Packaging Handbook*, New York, N.Y., Van Nostrand Reinhold.

4. Tummala, R. R. 1988. Ceramics in microelectronic packaging. *American Ceramic Society Bulletin* 67(4): pp. 752–58.

5. Keusseyan, R. L., Goeller, P. T., Page, J. P., Osborne, J. J., Nebe, W. J., and Polzer, E. K. 1990. A new method of metal-ceramic joining for advanced microelectronic packaging. *Proc. IEEE/ISHM'90 IEMT Symposium*, pp. 186–195.

6. Hey, A. W. 1990. Metallizing ceramic surfaces. *Joining of Ceramics*, ed. M. G. Nicholas, pp. 56–72, London, Chapman and Hall.

7. Bailey, G. L. J., and Watkins, H. C. 1952. The flow of liquid metals on solid metal surfaces and its relation to soldering, brazing, and hot-dip coating. *Journal of the Institute of Metals* 80: 57–76.

8. Bannos, T. S. 1984. The effect of furnace atmosphere composition on braze flow. *Heat Treatment of Metals* 2: 35–40.

9. Ambrose, J. C., Nicholas, M. G., and Stoneham, A. M. 1992. Dynamics of braze spreading. *Acta metall. mater.* 40 (10): 2483–2488.

10. Sahara, H. , Emoto, Y., and Otsuka, K. 1982. Improvement of metallization for alumina substrates. *Proc. 32nd IEEE Elec. Components Conf.*, pp. 32–35.

11. Murray, C. M., Letherman, G. L. , Bar-On, I., and Kellerman, D. W. 1989. The effect of brazing on the mechanical properties of cofired ceramic packages. *ISHM Procedings*, pp. 89–102, Baltimore, Md.

12. Rosebury, F. 1965. *Handbook of Electron Tube and Vacuum Techniques* p.334, Reading, Mass., Addison-Wesley.

13. Sidhu, G. S., and Mathew, R. 1967. Prevention of stress-corrosion cracking of Kovar material. *IEEE Transactions on Parts, Materials and Packaging*. PMP-4 (1): 30.

14. Weirick, L. J. 1976. Prevention of liquid-metal embrittlement and stress-corrosion cracking in Kovar leads. *Solid State Technology*, June, pp. 55–61.

15. Weirick, L. J. 1977. A metallurgical analysis of stress-corrosion cracking of Kovar package leads. *Electrochem. Conf. Proc.* pp. 130–132, Philadelphia, Pa.

16. Vaughan, J. G. 1980. Reliability of metallization procedures for Kovar lead frames. *Second Symp. on Design and Finishing of Printed Wiring and Hybrid Circuits*, San Francisco, Calif., pp. 1–20.

17. Rosengarth, K. W., Jr. 1984. Corrosion protection for semiconductor packaging. *Solid State Technology*, June, pp. 191–196.

18. Dogra, K. S. 1987. Catastrophic failure of hybrid leads. *Microstructural Science*, Vol. 16, eds. H. J. Cialoni, M. E. Blum, G. W. E. Johnson, and G. F. Vandervoort, pp. 41–51.

19. Chen, F-G. 1988. Influences of brazing temperature on Kovar leads. *Electronic Packaging and Production* 28(2):32–133.

20. Raffalovich, A. J. 1971. *IEEE Trans. on Parts, Materials, and Packaging*, Vol. PMP-7, No. 4, pp.155–162.

21. Baker, R. G., and Mendizza, A. 1963. *Electro-Technology* 72(10): 11–12.

22. Elkind, M. J., and Hughes, H. E. 1967. Prevention of stress-corrosion failure in iron-nickel-cobalt alloy semiconductor device leads, *Physics of Failure in Electronics* 5:447–495.

23. Fuerschbach, P. W. 1982. The effect of processing on environmental degradation of brazed and plated Kovar leads. Sandia National Laboratories Report No. SAND-2601.

24. Goldman, L. S. 1981. Mechanical optimization of brazed pins. *International Journal of Hybrid Microelectronics* 4(2):420-427.

25. Mazia, J., and Lashmore, D. S. 1987. Electroplated coatings. *Metals Handbook*, 9th ed. Vol. 13, *Corrosion*, ASM International, Metals Park, Ohio.

26. Cochran, W. G., and Cox, G. M. 1957. *Experimental Designs*, 2nd ed., New York, N.Y., Wiley.

27. Davies, O. L. (ed.) 1967. *The Design and Analysis of Industrial Experiments*, 2nd ed., New York, N.Y., Hafner.

28. Hicks, C. R. 1964. *Fundamental Concepts in the Design of Experiments*, New York, N.Y., Rinehart and Winston.

29. Felbeck, D. K., and Atkins, A. G. 1984. *Strength and Fracture of Engineering Solids* pp. 164–172, Englewood Cliffs, N.J., Prentice-Hall.

30. Reed-Hill, R. E. 1973. *Physical Metallurgy Principles*, 2nd. ed., pp. 541–549, New York, N.Y., D. Van Nostrand.

31. Siewert, T. A., and Heine, R. W. 1977. A recent look at the Ag-Cu-Ni system. *Metallurgical Transactions A* 8A: 515–518.

32. *IBM Technical Disclosure Bulletin*. 1986. 28(10):4638-4641.

33. ASTM B117-85. 1985. *Standard Method of Salt Spray (Fog) Testing*.

34. Abbott, W. H. 1987. Corrosion of porous gold plating in field and laboratory environments. *Plating and Surface Finishing* November: 72–75.

35. Clarke, M. 1975. Porosity and porosity tests. *Properties of Electrodeposits — Their Measurement and Significance*. eds. R. Sard, H. Leidheiser, Jr., and F. Ogburn, The Electrochemical Society, pp. 122–141, Princeton, N.J.

36. Weil, R. 1974. Structure, brightness and corrosion resistance of electrodeposits. *Plating* July: 654-661.